Contribution from the Department of Chemistry, Faculty of Engineering Science, Osaka University, Toyonaka, Osaka 560, Japan

Molecular Models of the Superconducting Chevrel Phases: Syntheses and Structures of $[Mo_6X_8(PEt_3)_6]$ and $[PPN][Mo_6X_8(PEt_3)_6]$ (X = S, Se; PPN = $(Ph_3P)_2N$)

Taro Saito,*[1a] Naohiro Yamamoto, Toshimi Nagase, Toshio Tsuboi, Kazuyo Kobayashi, Tsuneaki Yamagata, Hideo Imoto, and Kei Unoura[1b]

Received July 5, 1989

Hexanuclear molybdenum complexes $[Mo_6X_8(PEt_3)_6]$ (**1**, X = S; **2**, X = Se) have been prepared by magnesium reduction of the reaction products of $Mo_3X_7Cl_4$ with triethylphosphine. Treatment of the complexes with sodium amalgam followed by cation exchange with (PPN)Cl (PPN = bis(triphenylphosphine)nitrogen(1+)) gave $[PPN][Mo_6X_8(PEt_3)_6]$ (**3**, X = S; **4**, X = Se). The X-ray structure determinations have revealed that the Mo_6 octahedra of the 20-electron complexes **1** and **2** are very regular in contrast to those of the solid-state compounds Mo_6X_8. The average bond distances are Mo-Mo = 2.663 Å (**1**), 2.704 Å (**2**) and Mo-X = 2.445 Å (**1**), 2.560 Å (**2**). The one-electron-reduced complexes **3** and **4** are slightly distorted from regular octahedra due to the occupation of the e_g orbital. The average bond distances are Mo-Mo = 2.674 Å (**3**), 2.714 Å (**4**) and Mo-X = 2.458 Å (**3**), 2.570 Å (**4**). The electronic spectra of the neutral complexes indicate absorptions at 991 nm (**1**) and 1034 nm (**2**), which are assignable to a HOMO-LUMO transition. The cyclic voltammetry of **1** and **2** in THF solutions shows a quasi-reversible one-electron-oxidation wave and two one-electron-reduction waves. The space group, cell constants, number of observed reflections, R, and R_w are given as follows in that order. **1**: $R\bar{3}$, a = 17.460 (3) Å, c = 19.931 (6) Å, Z = 3, 1423, 0.039, 0.043. **2**: $P\bar{1}$, a = 13.036 (5) Å, b = 20.492 (6) Å, c = 12.208 (2) Å, α = 93.31 (3)°, β = 108.85 (1)°, γ = 88.85 (5)°, Z = 2, 7350, 0.046, 0.041. **3**: $C2/c$, a = 26.212 (9) Å, b = 18.040 (4) Å, c = 21.865 (8) Å, β = 114.87 (2)°, Z = 4, 6708, 0.060, 0.079. **4**: $C2/c$, a = 26.540 (5) Å, b = 18.117 (5) Å, c = 22.032 (4) Å, β = 115.39 (2)°, Z = 4, 5702, 0.067, 0.045.

Introduction

The structural chemistry of the superconducting Chevrel phases $M_xMo_6X_8$ (M = Pb, Sn, Cu, etc.; X = S, Se, Te)[2] has posed the interesting problems of the relationship between the shape of the octahedral Mo_6 cluster and the number of electrons in the cluster.[3] The Mo_6 cluster with 24 electrons is almost regular, and as the number of electrons decreases from 24 to 20, the Mo_6 octahedron becomes trigonally more elongated and the average Mo-Mo distance longer. The change of the chalcogen atom from sulfur to selenium also has the effect of diminishing the trigonal distortion of the octahedron. These tendencies were interpreted in terms of the net electron density in the metal cluster.[3] However, this argument was challenged by the different view that intercluster interactions were more structure determining than the electronic effect.[4] The problem may partly be solved if the structures of the molecular cluster complexes with the same Mo_6X_8 (X = S, Se) units are determined, because the intercluster interaction in such molecular clusters should be much smaller than in the solid-state compounds and the change of the structure would reflect major electronic effects.

We have found that the reductive condensation of the trinuclear molybdenum cluster chloro-sulfido complexes leads to the formation of $[Mo_6S_8(PEt_3)_6]$.[5] The present paper describes the syntheses and structures of a selenido analogue and one-electron-reduced complexes of the sulfido and selenido complexes. The results are discussed from the viewpoint of the electron-structure relationship.

Experimental Section

Reagents. $Mo_3X_7Cl_4$ (X = S, Se) were prepared by heating $MoCl_3$ with elemental sulfur or selenium in sealed Pyrex tubes according to the literature methods.[6] PEt_3 (Nippon Chemical Co. Ltd.) was used as received. The solvents were dried and distilled under dinitrogen.

Instruments. ^1H NMR spectra were measured by a JEOL FX100 spectrometer with tetramethylsilane (internal) reference, and infrared spectra were recorded by a Hitachi 295 spectrometer (4000-250 cm^{-1}). UV-vis spectra were obtained by Simadzu UV-265FS (300-900 nm) and Hitachi U-3400 spectrometers (900-2000 nm). XPS spectra were measured by a VG Scientific Escalab MkII instrument, and the binding energies were calibrated with C 1s = 284.6 eV.

Synthesis. Every operation was carried out under dinitrogen or argon. Rigorous exclusion of dioxygen was imperative to isolate the reduced cluster complexes **3** and **4**.

$[Mo_6S_8(PEt_3)_6]$ (1). A suspension of $Mo_3S_7Cl_4$ (1.0 g, 1.5 mmol) in PEt_3 (21.6% toluene solution, 9.8 mL, 15.3 mmol) was stirred at room temperature for 24 h. The solvent and excess triethylphosphine were removed under reduced pressure, THF (10 mL) and magnesium (74 mg, 3.1 mmol) were added to the residue, and the mixture was refluxed for 12 h. After cooling to room temperature, the solution was filtered and acetone (10 mL) was added to the filtrate, which was cooled at -20 °C. Solid product was filtered out, washed with acetone, and recrystallized from dichloromethane to give red-violet crystals; yield 32%. Anal. Calcd for $C_{36}H_{90}Mo_6P_6S_8$: C, 28.06; H, 5.89; Mo, 37.4; P, 12.1. Found: C, 28.06; H, 5.70; Mo, 38.9; P, 11.9. (Mo and P were analyzed by ICP spectrometry.)

$[Mo_6Se_8(PEt_3)_6]$ (2). A procedure for **1** was followed, using $Mo_3Se_7Cl_4$ to give blue crystals; yield 21%. Anal. Calcd for $C_{36}H_{90}Mo_6P_6Se_8$: C, 22.56; H, 4.73; Mo, 30.04. Found: C, 22.68; H, 4.69; Mo, 30.4.

$[PPN][Mo_6S_8(PEt_3)_6]$ (3). Complex **1** (0.1 g, 0.07 mmol) was treated with 1% Na-Hg (1.5 g, 0.07 mmol) in THF (10 mL) at room temperature for 15 min, and the solution was filtered into a flask containing (PPN)Cl (0.04 g, 0.07 mmol). The mixture was stirred for 24 h, filtered, concentrated, and cooled at 0 °C to give deep orange crystals; yield 49%. Anal. Calcd for $C_{72}H_{120}Mo_6NP_8S_8$: C, 41.58; H, 5.82; N, 0.67. Found: C, 41.92; H, 5.93; N, 0.64.

$[PPN][Mo_6Se_8(PEt_3)_6]$ (4). A procedure similar to that used for **3**, but using **2**, was followed to give deep red crystals; yield 36%. Anal. Calcd for $C_{72}H_{120}Mo_6NP_8Se_8$: C, 35.23; H, 4.93; N, 0.57. Found: C, 35.35; H, 4.83; N, 0.57.

X-ray Structure Determination. Single crystals of **1**, **3**, and **4** were grown from a tetrahydrofuran solution and those of **2** from a dichloromethane-acetone solution, and they were sealed in glass capillaries for the X-ray measurements. The crystals of **3** and **4** contained 1 mol of tetrahydrofuran as a crystallization solvent. The space group and the approximate cell dimensions of the crystals of **1**-**3** were determined from oscillation and Weissenberg photographs. The crystal of **4** was found to be isomorphous with the crystal of **3** from the cell dimensions determined

(1) (a) Present address: Department of Chemistry, Faculty of Science, The University of Tokyo, Hongo, Tokyo 113, Japan. (b) Department of Chemistry, Faculty of Science, Yamagata University, Yamagata 990, Japan.
(2) (a) Fischer, Ø., Maple, M. B., Eds. *Superconductivity in Ternary Compounds I*; Springer: Berlin, 1982. (b) Fischer, Ø. *Appl. Phys.* **1978**, *16*, 1. (c) Chevrel, R.; Gougeon, P.; Potel, M.; Sergent, M. J. *Solid State Chem.* **1985**, *57*, 25. (d) Chevrel, R.; Hirrien, M.; Sergent, M. *Polyhedron* **1986**, *5*, 87. (e) Perrin, A.; Perrin, C.; Sergent, M. *J. Less-Common Met.* **1988**, *137*, 241.
(3) (a) Yvon, K. Reference 2a, p 87. (b) Yvon, K. *Current Topics in Materials Science*; Kaldis, E., Ed.; North-Holland: Amsterdam, 1979; Vol. 3, p 53. (c) Yvon, K.; Paoli, A. *Solid State Commun.* **1977**, *24*, 41.
(4) Corbett, J. D. *J. Solid State Chem.* **1981**, *39*, 56.
(5) Saito, T.; Yamamoto, N.; Yamagata, T.; Imoto, H. *J. Am. Chem. Soc.* **1988**, *110*, 1646.
(6) (a) Opalovskii, A. A.; Fedorov, V. E.; Khaldoyanidi, K. A. *Dokl. Akad. Nauk SSSR* **1968**, *182*, 1095. (b) Fedorov, V. E.; Mishchenko, A. V.; Fedin, V. P. *Russ. Chem. Rev.* (*Engl. Transl.*) **1985**, *54*, 408.

0020-1669/90/1329-0764$02.50/0

Table I. Crystal Parameters and X-ray Diffraction Data for **1–4**

	1	2	3	4
formula	$C_{36}H_{90}Mo_6P_6S_8$	$C_{36}H_{90}Mo_6P_6Se_8$	$C_{76}H_{128}Mo_6NP_8S_8$	$C_{76}H_{128}Mo_6NP_8Se_8$
fw	1541.12	1916.27	2151.82	2526.97
space group	$R\bar{3}$	$P\bar{1}$	$C2/c$	$C2/c$
a, Å	17.460 (3)	13.036 (5)	26.212 (9)	26.540 (5)
b, Å		20.492 (6)	18.040 (4)	18.117 (5)
c, Å	19.931 (6)	12.208 (2)	21.865 (8)	22.032 (4)
α, deg		93.31 (3)		
β, deg		108.85 (1)	114.87 (2)	115.39 (2)
γ, deg		88.85 (5)		
V, Å^3	5262 (2)	3081 (2)	9380 (6)	9570 (4)
Z	3	2	4	4
μ, cm^{-1}	14.02	60.2	11.0	39.28
abs cor[a]	1.00–1.23	1.00–1.48	1.00–1.11	1.00–1.62
obsd reflcns[b]	1423, ($>6\sigma$)	7350, ($>6\sigma$)	6708, ($>6\sigma$)	5702, ($>6\sigma$)
R, R_w[c]	0.039, 0.043	0.041, 0.046	0.058, 0.079	0.066, 0.043

[a] Relative absorption correction coefficient (empirical ϕ-scan method). [b] Number of observed reflections with the criterion for the observations in parentheses. [c] $w = 1/\sigma^2(F_o)$.

Table II. Fractional Atomic Coordinates and Equivalent Isotropic Thermal Parameters[a] for $[Mo_6S_8(PEt_3)_6]$ (**1**)

atom	x	y	z	U_{eq}, Å^2
Mo	0.03505 (6)	0.10021 (5)	0.05450 (4)	0.0234 (3)
S(1)	0.0000	0.0000	0.1499 (2)	0.034 (1)
S(2)	−0.1194 (2)	0.0638 (2)	0.0504 (1)	0.031 (1)
P	0.0877 (2)	0.2375 (2)	0.1254 (1)	0.036 (1)
C(1)	0.1622 (7)	0.2441 (7)	0.1954 (5)	0.051 (5)
C(2)	0.1958 (9)	0.3291 (9)	0.2394 (6)	0.083 (8)
C(3)	0.1491 (8)	0.3436 (6)	0.0802 (6)	0.050 (5)
C(4)	0.2354 (8)	0.3571 (7)	0.0487 (6)	0.064 (6)
C(5)	−0.0002 (8)	0.2503 (8)	0.1662 (6)	0.057 (6)
C(6)	−0.0542 (8)	0.1819 (10)	0.2181 (6)	0.068 (7)

[a] The isotropic equivalent thermal parameters are defined as $U_{eq} = (1/3)\sum_{i,j}U_{ij}a_i^*a_j^*(\mathbf{a}_i\cdot\mathbf{a}_j)$.

by a diffractometer and intensities of the low-angle reflections. X-ray measurements of the crystals were performed at 20 °C on a Rigaku AFC-4 diffractometer equipped with a Rotaflex rotating anode X-ray generator (the crystals of **1–3**) or a Rigaku AFC-6 diffractometer with a sealed normal-focus X-ray tube (the crystal of **4**). The radiation used was Mo Kα monochromatized with graphite (0.71069 Å). The intensity data of all crystals did not indicate any decay, and data were corrected for the Lp factor and empirically for the absorption. The positions of the heavy atoms (molybdenum, chalcogen, and phosphorus atoms) of **1–3** were determined by direct methods using MULTAN78. As the starting positional parameters of **4**, the same coordinates of the heavy atoms as found in **3** were used. The carbon and nitrogen atoms were located on the Fourier maps, and all non-hydrogen atoms were refined by the full-matrix least-squares method. In the last stage of the refinement of **1**, hydrogen atoms were included at calculated fixed positions. Hydrogen atoms were not included in the calculations of **2–4**.

The tetrahydrofuran in the crystals of **3** and **4** was distributed in two neighboring positions, which were related to each other by inversion symmetry. Since its oxygen atom could not be distinguished from the carbon atoms, the tetrahydrofuran molecule was treated as a C_5 ring. In the refinement of **3**, the positions of the atoms of tetrahydrofuran were located at the fixed positions found on the Fourier map. In the case of **4**, the atomic positions of the tetrahydrofuran molecule were determined from the Fourier map so that it had the shape of a planar pentagon with the C–C distance of 1.50 Å.

The comparison of the observed and calculated structure factors of the strong reflections of **4** showed an obvious effect of extinction, and the extinction parameter γ was introduced in the refinement of **4** as $|F_c(\text{cor})| = |F_c(\text{raw})|/(1 + \gamma Lp|F_c(\text{raw})|^2)^{1/2}$.

The crystallographic data are given in Table I, and other details, in the supplementary material. The final atomic parameters of **1–4** are listed in Tables II–V.

Electrochemistry. Voltammetry was performed on a HECS-312B polarographic analyzer with a HECS-321B function generator (Huso Co.). A three-electrode cell consisting of a glassy-carbon-disk working electrode (diameter 0.3 cm), a Pt-coil auxiliary electrode, and a saturated sodium calomel reference electrode (NaSCE) was used for the measurements. The ferrocene/ferrocenium (Fc/Fc^+) redox couple was used as a standard of potential.

Thin-layer coulometry was carried out on a HECS-312B polarographic analyzer coupled with a HECS-978 coulometer (Huso Co.) by

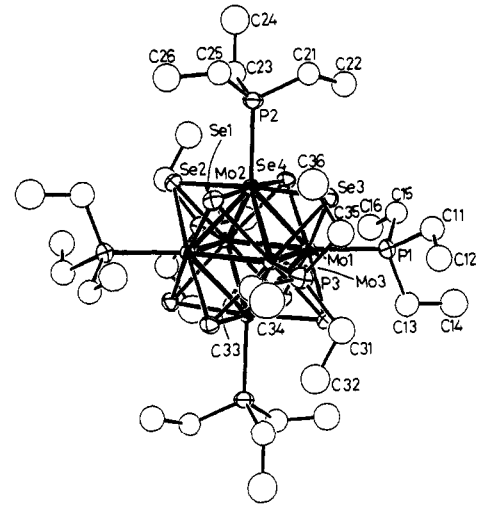

Figure 1. ORTEP drawing of $[Mo_6Se_8(PEt_3)_6]$ (**2A**). All hydrogen atoms are omitted for clarity.

using a micrometer thin-layer electrochemical cell with a glassy-carbon disk (diameter 0.3 cm) as a working electrode.[7] Tetrabutylammonium tetrafluoroborate (Nakarai Tesque Inc., specially prepared reagent for polarography) was used as the supporting electrolyte without further purification. Reagent grade dichloromethane (Wako Pure Chemicals Industries) was refluxed over CaH_2 for several hours and then was fractionally distilled. Reagent grade tetrahydrofuran (Wako Pure Chemicals Industries) was refluxed over CuCl for 30 min and then purified by fractional distillation.

Results

Synthesis. As described in our previous communication,[5] the hexanuclear molybdenum complex **1** was initially prepared from an isolated trinuclear cluster complex coordinated with both triethylphosphine and methanol. We found subsequently that **1** was more conveniently prepared directly by the reduction with magnesium of the reaction product of $Mo_3S_7Cl_4$ with triethylphosphine (eq 1). The selenido analogue **2** was also prepared

$$Mo_3X_7Cl_4 + 8PEt_3 \rightarrow \text{“}[Mo_3X_4Cl_4(PEt_3)_5]\text{”} + 3XPEt_3$$

$$2\text{“}[Mo_3X_4Cl_4(PEt_3)_5]\text{”} + 4Mg \rightarrow [Mo_6X_8(PEt_3)_6] + 4MgCl_2 + 4PEt_3 \quad (1)$$

by the similar procedure. Both **1** and **2** are rather stable toward air, but the reduced clusters **3** and **4** are extremely sensitive to air oxidation and return to the neutral cluster complexes readily. Therefore, the reductions with sodium amalgam followed by the cation exchange by PPN salt were carried out under argon with utmost care to exclude trace oxygen.

(7) Hubbard, A. T.; Anson, F. C. *Electroanalytical Chemistry*; Bard, A.J., Ed.; Marcel Dekker: New York, 1970; Vol. 4, p 129.

Table III. Fractional Atomic Coordinates and Equivalent Isotropic Thermal Parameters[a] for $[Mo_6Se_8(PEt_3)_6]$ (**2**)

atom	x	y	z	U_{eq}, Å^2
Mo(1)	−0.09696 (8)	0.01051 (4)	0.08857 (8)	0.0231 (3)
Mo(2)	0.08746 (8)	0.06965 (4)	0.09178 (8)	0.0223 (3)
Mo(3)	−0.08371 (8)	0.06128 (4)	−0.10576 (8)	0.0229 (3)
Se(1)	0.09549 (10)	0.11431 (5)	−0.09717 (10)	0.0325 (4)
Se(2)	0.25336 (9)	−0.00187 (5)	0.10203 (10)	0.0306 (4)
Se(3)	−0.08737 (10)	0.13432 (5)	0.06999 (10)	0.0323 (4)
Se(4)	0.06971 (10)	0.01790 (5)	0.27035 (10)	0.0306 (4)
P(1)	−0.2299 (3)	0.0233 (2)	0.2018 (3)	0.037 (1)
P(2)	0.2068 (3)	0.1584 (1)	0.2220 (3)	0.034 (1)
P(3)	−0.1935 (3)	0.1418 (1)	−0.2502 (3)	0.038 (1)
Mo(1b)	0.39883 (8)	0.49047 (4)	0.08182 (9)	0.0268 (3)
Mo(2b)	0.57071 (8)	0.56869 (4)	0.10927 (9)	0.0276 (4)
Mo(3b)	0.40688 (8)	0.56266 (4)	−0.09375 (9)	0.0268 (3)
Se(3b)	0.55975 (10)	0.49628 (6)	0.26942 (10)	0.0355 (4)
Se(4b)	0.24892 (10)	0.48555 (6)	−0.11519 (11)	0.0363 (5)
Se(1b)	0.42544 (10)	0.36654 (5)	0.06214 (11)	0.0349 (4)
Se(2b)	0.38241 (10)	0.61523 (5)	0.09214 (11)	0.0378 (5)
P(1b)	0.2649 (3)	0.4799 (2)	0.1922 (3)	0.040 (1)
P(2b)	0.6654 (3)	0.6617 (2)	0.2499 (3)	0.048 (1)
P(3b)	0.2831 (3)	0.6436 (2)	−0.2253 (3)	0.040 (1)
C(11)	−0.298 (1)	0.6436 (2)	−0.2253 (3)	0.040 (1)
C(11)	−0.298 (1)	0.104 (1)	0.199 (1)	0.054 (4)
C(12)	−0.368 (1)	0.122 (1)	0.077 (1)	0.060 (4)
C(13)	−0.346 (1)	−0.034 (1)	0.152 (1)	0.054 (4)
C(14)	−0.426 (1)	−0.029 (1)	0.226 (1)	0.075 (5)
C(15)	−0.173 (1)	0.015 (1)	0.361 (1)	0.048 (3)
C(16)	−0.130 (1)	−0.055 (1)	0.392 (1)	0.066 (4)
C(21)	0.139 (1)	0.224 (1)	0.284 (1)	0.045 (3)
C(22)	0.078 (1)	0.198 (1)	0.365 (1)	0.058 (4)
C(23)	0.310 (1)	0.126 (1)	0.349 (1)	0.052 (3)
C(24)	0.388 (1)	0.178 (1)	0.434 (1)	0.078 (5)
C(25)	0.282 (1)	0.211 (1)	0.155 (1)	0.050 (3)
C(26)	0.371 (1)	0.173 (1)	0.119 (1)	0.068 (4)
C(31)	−0.341 (1)	0.125 (1)	−0.319 (1)	0.058 (4)
C(32)	−0.361 (1)	0.061 (1)	−0.401 (1)	0.071 (4)
C(33)	−0.140 (1)	0.061 (1)	−0.401 (1)	0.071 (4)
C(33)	−0.140 (1)	0.149 (1)	−0.372 (1)	0.055 (4)
C(34)	−0.204 (2)	0.196 (1)	−0.466 (2)	0.097 (6)
C(35)	−0.210 (1)	0.226 (1)	−0.197 (1)	0.059 (4)
C(36)	−0.097 (1)	0.263 (1)	−0.156 (1)	0.079 (5)
C(11b)	0.146 (1)	0.535 (1)	0.149 (1)	0.057 (4)
C(12b)	0.067 (1)	0.533 (1)	0.221 (1)	0.078 (5)
C(13b)	0.203 (1)	0.398 (1)	0.184 (1)	0.055 (4)
C(14b)	0.134 (1)	0.375 (1)	0.060 (1)	0.063 (4)
C(15b)	0.321 (1)	0.492 (1)	0.354 (1)	0.064 (4)
C(16b)	0.359 (1)	0.565 (1)	0.391 (1)	0.078 (5)
C(21b)	0.580 (1)	0.734 (1)	0.263 (1)	0.069 (4)
C(22b)	0.537 (1)	0.771 (1)	0.153 (2)	0.083 (5)
C(23b)	0.778 (1)	0.697 (1)	0.215 (1)	0.068 (4)
C(24b)	0.841 (2)	0.754 (1)	0.300 (2)	0.099 (6)
C(25b)	0.720 (1)	0.645 (1)	0.405 (1)	0.073 (5)
C(26b)	0.813 (2)	0.592 (1)	0.427 (2)	0.096 (6)
C(31b)	0.193 (1)	0.696 (1)	−0.167 (1)	0.057 (4)
C(32b)	0.109 (1)	0.658 (1)	−0.137 (1)	0.072 (4)
C(33b)	0.190 (1)	0.604 (1)	−0.360 (1)	0.059 (4)
C(34b)	0.113 (2)	0.649 (1)	−0.444 (2)	0.090 (6)
C(35b)	0.350 (1)	0.711 (1)	−0.273 (1)	0.052 (3)
C(36b)	0.417 (1)	0.686 (1)	−0.352 (1)	0.069 (4)

[a] See the footnote *a* of Table II.

Structure. The structure of complex **1** has been communicated,[5] but the detailed structural data are given for the purpose of comparison with the other cluster compounds in Tables II and VI. Complex **2** crystallizes in the triclinic space group $P\bar{1}$, and there are two independent molecules, **2A** and **2B**, in a unit cell. The selected interatomic distances and angles are listed in Table VII. Figure 1 illustrates the structure of **2A**, which is virtually identical with that of **2B**. The average Mo–Mo bond distance for **2** is longer than that for **1** by 0.041 (1) Å; namely the selenido cluster is a little larger than the sulfido cluster.

Just like that of the sulfido analogue **1**, the structure of **2** is characterized by its regular octahedral framework of six molybdenum atoms that bond to each other with the Mo–Mo bond distances ranging from 2.697 (1) to 2.708 (1) Å. The Mo–Mo–Mo bond angles also exhibit its regular octahedral structure. There is no indication that the structures of **1** and **2** are trigonally distorted like the solid-state compounds Mo_6S_8 and Mo_6Se_8, whose clusters are trigonally elongated,[8] or like the 20-electron niobium clusters in $Nb_6I_{11}H$[9] and $CsNb_6I_{11}$,[10] which are trigonally twisted. In **1** and **2**, it is very improbable that orientational disorder of trigonally distorted clusters leads to the seemingly regular shape because such trigonal distortions are likely to be frozen in the structure of **1**, where the cluster is located on the crystallographic 3-fold axis.

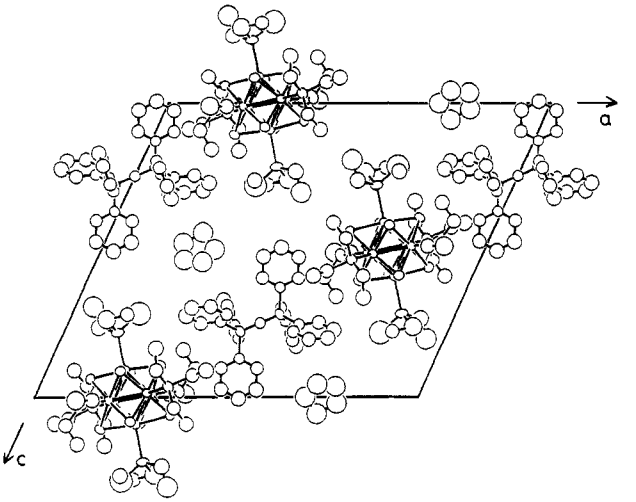

Figure 2. ORTEP drawing of the unit cell of $[PPN][Mo_6Se_8(PEt_3)_6]$ (**3**) projected on the *ac* plane.

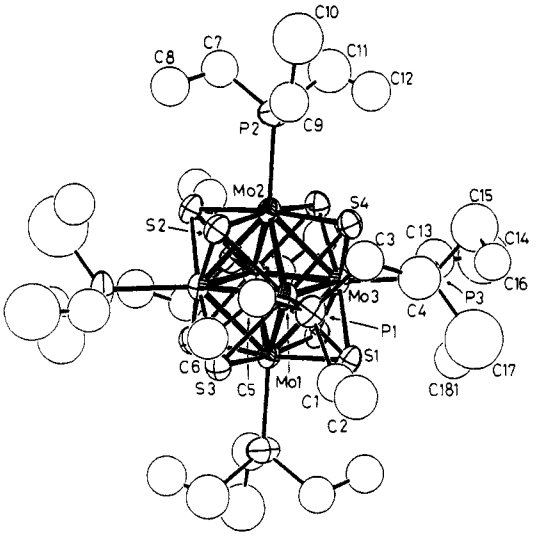

Figure 3. ORTEP drawing of **3**, showing a $[Mo_6S_8(PEt_3)_6]^-$ ion.

One-electron reduction of **1** formed **3**, which crystallized in the monoclinic space group $C2/c$. The selected interatomic distances and angles are listed in Table VIII. The unit cell structure is illustrated in Figure 2, and the molecular structure, in Figure 3. The average Mo–Mo bond distance 2.674 (1) Å is a little (0.011 (1) Å) longer than that of the neutral cluster **1**. The Mo–μ_3-S bond distances for **2** are also 0.013 (2) Å longer than those for **1**.

The selenido analogue **4** crystallizes in the monoclinic space group $C2/c$ and is isomorphous with **3**. The selected interatomic distances and angles are listed in Table IX. There is some disorder of tetrahydrofuran and of the ethyl groups of the triethylphosphine ligands. The overall structure is slightly distorted, and the average Mo–Mo and Mo–Se bond distances are longer than those for **2**.

(8) Bars, O.; Guillevic, J.; Grandjean, D. *J. Solid State Chem.* **1973**, *6*, 48.
(9) Imoto, H.; Simon, A. *Inorg. Chem.* **1982**, *21*, 308.
(10) Imoto, H.; Corbett, J. D. *Inorg. Chem.* **1980**, *19*, 1241.

Table IV. Fractional Atomic Coordinates and (Equivalent) Isotropic Thermal Parameters[a] for $[PPN][Mo_6S_8(PEt_3)_6]\cdot THF$ (**3**)

atom	x	y	z	$U_{eq/iso}$, Å^2
Mo(1)	0.71252 (3)	0.33266 (4)	0.51454 (4)	0.0380 (3)
Mo(2)	0.80252 (3)	0.31433 (5)	0.48869 (4)	0.0396 (3)
Mo(3)	0.79606 (4)	0.24487 (5)	0.59324 (4)	0.0395 (3)
S(1)	0.7088 (1)	0.2630 (1)	0.6090 (1)	0.049 (1)
S(2)	0.72109 (11)	0.38943 (14)	0.41709 (13)	0.0474 (11)
S(3)	0.6247 (1)	0.2716 (1)	0.4384 (1)	0.048 (1)
S(4)	0.80637 (11)	0.37951 (14)	0.58850 (13)	0.0485 (11)
P(1)	0.6639 (1)	0.4466 (2)	0.5349 (2)	0.053 (1)
P(2)	0.8696 (1)	0.4122 (2)	0.4800 (2)	0.069 (2)
P(3)	0.8588 (1)	0.2348 (2)	0.7185 (1)	0.067 (1)
P(4)	0.04225 (12)	0.22643 (14)	0.22119 (14)	0.0484 (12)
N	0.0000	0.1980 (6)	0.2500	0.055 (3)
C(1)	0.6140 (6)	0.4265 (8)	0.5734 (7)	0.090 (4)
C(2)	0.5843 (6)	0.4933 (9)	0.5894 (8)	0.113 (5)
C(3)	0.7141 (6)	0.5220 (8)	0.5906 (7)	0.093 (4)
C(4)	0.7400 (6)	0.4911 (9)	0.6640 (8)	0.114 (5)
C(5)	0.6237 (5)	0.5086 (8)	0.4620 (7)	0.086 (4)
C(6)	0.5725 (6)	0.4698 (8)	0.4088 (7)	0.100 (5)
C(7)	0.8853 (6)	0.4147 (8)	0.4047 (7)	0.094 (4)
C(8)	0.8330 (6)	0.4214 (8)	0.3410 (8)	0.104 (5)
C(9)	0.8458 (6)	0.5064 (8)	0.4888 (7)	0.101 (5)
C(10)	0.889 (1)	0.570 (1)	0.489 (1)	0.163 (8)
C(11)	0.9546 (7)	0.4008 (10)	0.5504 (9)	0.132 (6)
C(12)	0.955 (1)	0.403 (2)	0.606 (2)	0.110 (10)
C(13)	0.9138 (7)	0.1643 (9)	0.7349 (8)	0.118 (6)
C(14)	0.953 (1)	0.147 (1)	0.805 (1)	0.203 (10)
C(15)	0.903 (1)	0.320 (1)	0.763 (1)	0.158 (8)
C(16)	0.855 (1)	0.365 (2)	0.779 (1)	0.092 (9)
C(17)	0.825 (1)	0.213 (2)	0.782 (2)	0.252 (15)
C(181)[b]	0.817 (2)	0.153 (2)	0.766 (2)	0.112 (11)
C(182)[b]	0.785 (2)	0.179 (3)	0.778 (2)	0.150 (16)
C(19)	0.0647 (4)	0.3204 (6)	0.2443 (5)	0.054 (3)
C(20)	0.0378 (4)	0.3774 (6)	0.1983 (6)	0.063 (3)
C(21)	0.0548 (5)	0.4529 (7)	0.2222 (7)	0.079 (4)
C(22)	0.0954 (6)	0.4648 (8)	0.2844 (8)	0.094 (4)
C(23)	0.1218 (6)	0.4085 (9)	0.3278 (8)	0.105 (5)
C(24)	0.1062 (5)	0.3326 (7)	0.3087 (6)	0.077 (4)
C(25)	0.0111 (4)	0.2197 (6)	0.1296 (5)	0.054 (3)
C(26)	0.0481 (5)	0.2302 (7)	0.0982 (6)	0.075 (4)
C(27)	0.0237 (6)	0.2256 (8)	0.0266 (7)	0.093 (4)
C(28)	−0.0335 (7)	0.2153 (9)	−0.0062 (8)	0.105 (5)
C(29)	−0.0689 (6)	0.2077 (8)	0.0246 (8)	0.105 (5)
C(30)	−0.0459 (5)	0.2086 (7)	0.0970 (7)	0.081 (4)
C(31)	0.1039 (4)	0.1672 (6)	0.2546 (5)	0.059 (3)
C(32)	0.0976 (5)	0.1001 (7)	0.2799 (6)	0.070 (3)
C(33)	0.1473 (6)	0.0509 (8)	0.3053 (7)	0.093 (4)
C(34)	0.1952 (6)	0.0743 (9)	0.3014 (8)	0.103 (5)
C(35)	0.2007 (7)	0.1413 (9)	0.2737 (8)	0.110 (5)
C(36)	0.1533 (6)	0.1910 (8)	0.2482 (7)	0.089 (4)
C(37)[c]	0.2944	0.2500	0.5000	0.19
C(38)[c]	0.2722	0.2333	0.4643	0.19
C(39)[c]	0.2444	0.2250	0.4429	0.19
C(40)[c]	0.2222	0.2133	0.4571	0.19
C(41)[c]	0.2056	0.2250	0.4786	0.19

[a] The molybdenum, sulfur, and phosphorus atoms were refined anisotropically. See footnote *a* of Table II. [b] A methyl carbon atom occupies two sites, C(181) and C(182). The occupancy factors of these sites were fixed as 0.5. [c] These atoms were of the disordered THF molecule and were not refined.

Table V. Fractional Atomic Coordinates and (Equivalent) Isotropic Thermal Parameters[a] for $[PPN][Mo_6Se_8(PEt_3)_6]\cdot THF$ (**4**)

atom	x	y	z	$U_{eq/iso}$, Å^2
Mo(1)	0.71269 (6)	0.33347 (10)	0.51523 (8)	0.0366 (10)
Mo(2)	0.80232 (6)	0.31485 (10)	0.48804 (8)	0.0375 (10)
Mo(3)	0.79724 (6)	0.24465 (10)	0.59431 (7)	0.0377 (10)
Se(1)	0.70944 (7)	0.26350 (12)	0.61436 (8)	0.0444 (11)
Se(2)	0.71919 (7)	0.39516 (11)	0.41361 (9)	0.0430 (12)
Se(3)	0.62018 (7)	0.27306 (11)	0.43668 (9)	0.0456 (11)
Se(4)	0.80954 (7)	0.38474 (12)	0.59251 (10)	0.0455 (12)
P(1)	0.6633 (2)	0.4462 (3)	0.5354 (3)	0.048 (3)
P(2)	0.8681 (2)	0.4132 (3)	0.4775 (3)	0.062 (4)
P(3)	0.8616 (2)	0.2344 (4)	0.7198 (2)	0.061 (3)
P(4)	0.5406 (2)	0.2709 (3)	0.7197 (2)	0.047 (3)
N	0.5000	0.2975 (10)	0.7500	0.044 (6)
C(1)	0.6100 (7)	0.4230 (11)	0.5689 (9)	0.063 (6)
C(2)	0.5824 (7)	0.4910 (12)	0.5825 (9)	0.085 (7)
C(3)	0.707 (1)	0.520 (1)	0.590 (1)	0.090 (7)
C(4)	0.734 (1)	0.491 (1)	0.666 (1)	0.089 (7)
C(5)	0.6260 (7)	0.5102 (11)	0.4653 (9)	0.063 (6)
C(6)	0.5752 (7)	0.4728 (10)	0.4078 (9)	0.057 (6)
C(7)	0.884 (1)	0.414 (1)	0.403 (1)	0.079 (7)
C(8)	0.8319 (7)	0.4289 (11)	0.3409 (9)	0.067 (6)
C(9)	0.846 (1)	0.511 (1)	0.486 (1)	0.073 (7)
C(10)	0.886 (1)	0.564 (2)	0.480 (1)	0.149 (11)
C(11)	0.948 (1)	0.403 (2)	0.531 (2)	0.163 (12)
C(12)	0.955 (1)	0.414 (2)	0.590 (2)	0.207 (15)
C(13)	0.920 (1)	0.160 (1)	0.739 (1)	0.084 (7)
C(14)	0.953 (1)	0.142 (2)	0.806 (1)	0.151 (11)
C(15)	0.905 (1)	0.319 (1)	0.763 (1)	0.131 (10)
C(161)[b]	0.854 (1)	0.367 (2)	0.778 (2)	0.052 (11)
C(162)[b]	0.956 (2)	0.337 (2)	0.731 (2)	0.101 (16)
C(17)	0.831 (1)	0.216 (2)	0.779 (1)	0.161 (13)
C(18)	0.804 (1)	0.165 (2)	0.776 (2)	0.215 (17)
C(19)	0.5106 (6)	0.2785 (9)	0.6317 (7)	0.041 (5)
C(20)	0.5451 (7)	0.2731 (12)	0.5972 (9)	0.081 (7)
C(21)	0.517 (1)	0.274 (1)	0.526 (1)	0.099 (8)
C(22)	0.460 (1)	0.285 (1)	0.489 (1)	0.097 (8)
C(23)	0.425 (1)	0.292 (1)	0.525 (1)	0.092 (8)
C(24)	0.453 (1)	0.289 (1)	0.598 (1)	0.084 (7)
C(25)	0.5624 (6)	0.1752 (10)	0.7401 (9)	0.043 (5)
C(26)	0.6067 (7)	0.1567 (12)	0.8061 (9)	0.066 (6)
C(27)	0.619 (1)	0.080 (1)	0.822 (1)	0.085 (8)
C(28)	0.590 (1)	0.030 (1)	0.777 (1)	0.076 (7)
C(29)	0.548 (1)	0.044 (1)	0.715 (1)	0.078 (7)
C(30)	0.5349 (6)	0.1181 (11)	0.6939 (8)	0.048 (5)
C(31)	0.6017 (7)	0.3300 (11)	0.7523 (8)	0.052 (5)
C(32)	0.6526 (7)	0.3038 (10)	0.7460 (8)	0.064 (6)
C(33)	0.701 (1)	0.357 (1)	0.774 (1)	0.091 (8)
C(34)	0.694 (1)	0.423 (1)	0.798 (1)	0.087 (7)
C(35)	0.6442 (8)	0.4459 (11)	0.8008 (9)	0.080 (7)
C(36)	0.5947 (7)	0.4026 (11)	0.7753 (9)	0.062 (6)
C(37)[c]	0.2500	0.3202	0.5000	0.323
C(38)[c]	0.2049	0.2717	0.4517	0.323
C(39)[c]	0.2221	0.1932	0.4701	0.323
C(40)[c]	0.2779	0.1932	0.5299	0.323
C(41)[c]	0.2951	0.2717	0.5483	0.323

[a] The molybdenum, selenium, and phosphorus atoms were refined anisotropically. [b] A methyl carbon atom occupies two sites, C(181) and C(182). The occupancy factors of these sites were fixed as 0.5. [c] These atoms were of the disordered THF molecule and were not refined.

The pertinent bond distances of the relevant cluster compounds are listed in Table X.

Spectra. (a) Electronic Spectra. The cluster complexes exhibit characteristic absorptions in the visible and near-infrared regions. The peak positions and intensities are given in Table XI. The lower energy bands have shoulders, and the higher energy bands are split in the case of the selenido derivatives.

(b) XPS. The peak positions in the X-ray photoelectron spectra of the complexes **1** and **2** are shown in Table XI. The valence band spectra will be discussed elsewhere in relation to the $X\alpha$ calculation of a model system.[11]

(11) Imoto, H.; Adachi, H.; Saito, T. To be published.

Table VI. Interatomic Distances (Å) and Angles (deg) for $[Mo_6S_8(PEt_3)_6]$ (**1**)[a]

Mo–Mo^{ii}	3.766 (1)	Mo–Mo^{iii}	2.664 (1)
Mo–Mo^{iv}	2.662 (1)	Mo–S(1)	2.446 (2)
Mo–S(2)	2.444 (3)	Mo–P	2.527 (3)
Mo^{iii}–S(2)	2.439 (3)	Mo^{vi}–S(2)	2.449 (3)
Mo^{iii}–Mo–Mo^{vi}	59.98 (3)	Mo^{iii}–Mo–Mo^{iv}	90.0
Mo^{iv}–Mo–S(2)	117.14 (8)	Mo^{vi}–Mo–S(2)	57.15 (7)
Mo–S(2)–Mo^{iii}	66.13 (8)	Mo^{vi}–Mo–P	135.38 (8)

[a] Equivalent positions: (ii) $-x, -y, -z$; (iii) $-y, x-y, z$; (iv) $y, -x+y, -z$; (v) $-x+y, -x, z$; (vi) $x-y, x, -z$.

Electrochemistry. The cyclic voltammograms of the cluster complexes **1** and **2** were measured in dichloromethane and THF

Table VII. Interatomic Distances (Å) and Angles (deg) for $[Mo_6Se_8(PEt_3)_6]$ (**2A**, **2B**)[a]

Mo(1)–Mo(1)′	3.825 (1)	Mo(1b)–Mo(1b)′	3.826 (1)
Mo(2)–Mo(2)′	3.820 (1)	Mo(2b)–Mo(2b)′	3.821 (1)
Mo(3)–Mo(3)′	3.824 (1)	Mo(3b)–Mo(3b)′	3.817 (1)
Mo(1)–Mo(2)	2.702 (1)	Mo(1b)–Mo(2b)	2.702 (1)
Mo(1)–Mo(3)	2.701 (1)	Mo(1b)–Mo(3b)	2.704 (1)
Mo(1)–Mo(2)′	2.704 (1)	Mo(1b)–Mo(2b)′	2.706 (1)
Mo(1)–Mo(3)′	2.708 (1)	Mo(1b)–Mo(3b)′	2.700 (1)
Mo(2)–Mo(3)	2.705 (1)	Mo(2b)–Mo(3b)	2.697 (1)
Mo(2)–Mo(3)′	2.701 (1)	Mo(2b)–Mo(3b)′	2.704 (1)
Mo(1)–Se(3)	2.570 (2)	Mo(1b)–Se(3b)	2.556 (2)
Mo(1)–Se(4)	2.555 (2)	Mo(1b)–Se(4b)	2.561 (2)
Mo(1)–Se(1)′	2.566 (2)	Mo(1b)–Se(1b)	2.564 (2)
Mo(1)–Se(2)′	2.550 (2)	Mo(1b)–Se(2b)	2.561 (2)
Mo(2)–Se(1)	2.564 (2)	Mo(2b)–Se(1b)′	2.556 (2)
Mo(2)–Se(2)	2.561 (2)	Mo(2b)–Se(2b)	2.565 (2)
Mo(2)–Se(3)	2.559 (2)	Mo(2b)–Se(3b)	2.563 (2)
Mo(2)–Se(4)	2.556 (2)	Mo(2b)–Se(4b)′	2.562 (2)
Mo(3)–Se(1)	2.565 (2)	Mo(3b)–Se(1b)′	2.559 (2)
Mo(3)–Se(3)	2.557 (2)	Mo(3b)–Se(3b)′	2.555 (2)
Mo(3)–Se(2)′	2.560 (2)	Mo(3b)–Se(2b)	2.566 (2)
Mo(3)–Se(4)′	2.560 (2)	Mo(3b)–Se(4b)	2.558 (2)
Mo(1)–P(1)	2.544 (3)	Mo(1b)–P(1b)	2.546 (4)
Mo(2)–P(2)	2.538 (3)	Mo(2b)–P(2b)	2.541 (4)
Mo(3)–P(3)	2.548 (3)	Mo(3b)–P(3b)	2.543 (4)
Mo(2)–Mo(1)–Mo(3)	60.07 (3)	Mo(2b)–Mo(1b)–Mo(3b)	59.86 (4)
Mo(3)–Mo(1)–Mo(3)′	89.98 (4)	Mo(3b)–Mo(1b)–Mo(3b)′	89.86 (4)
Mo(1)–Mo(2)–Se(1)	118.14 (5)	Mo(1b)–Mo(2b)–Se(3b)	58.02 (4)
Mo(3)–Mo(2)–Se(1)	58.20 (4)	Mo(3b)–Mo(2b)–Se(3b)	118.11 (5)
Mo(2)–Se(1)–Mo(3)	63.65 (4)	Mo(2b)′–Se(1b)–Mo(3b)′	63.64 (4)
Mo(2)–Mo(1)–P(1)	136.34 (9)	Mo(2b)–Mo(1b)–P(1b)	134.04 (9)

[a] Prime indicates an atom with equivalent position coordinates $-x, -y, -z$.

Table VIII. Interatomic Distances (Å) and Angles (deg) for $[PPN][Mo_6S_8(PEt_3)_6]$ (**3**)[a]

Mo(1)–Mo(1)′	3.770 (1)	Mo(2)–Mo(2)′	3.789 (1)
Mo(3)–Mo(3)′	3.770 (1)	Mo(1)–Mo(2)	2.668 (1)
Mo(1)–Mo(3)	2.664 (1)	Mo(1)–Mo(2)′	2.677 (1)
Mo(1)–Mo(3)′	2.667 (1)	Mo(2)–Mo(3)	2.674 (1)
Mo(2)–Mo(3)′	2.671 (1)	Mo(1)–S(1)	2.454 (3)
Mo(1)–S(2)	2.458 (3)	Mo(1)–S(3)	2.462 (3)
Mo(1)–S(4)	2.457 (3)	Mo(2)–S(1)′	2.462 (3)
Mo(2)–S(2)	2.456 (3)	Mo(2)–S(3)′	2.454 (3)
Mo(2)–S(4)	2.444 (3)	Mo(3)–S(1)	2.473 (3)
Mo(3)–S(2)′	2.457 (3)	Mo(3)–S(3)′	2.468 (3)
Mo(3)–S(4)	2.451 (3)	Mo(1)–P(1)	2.554 (3)
Mo(2)–P(2)	2.556 (4)	Mo(3)–P(3)	2.540 (4)
Mo(2)–Mo(1)–Mo(3)	60.21 (3)	Mo(3)–Mo(1)–Mo(3)′	90.00 (4)
Mo(2)–Mo(1)–S(1)	117.78 (7)	Mo(2)′–Mo(1)–S(1)	57.14 (7)
Mo(1)–S(1)–Mo(2)′	66.01 (8)	Mo(2)–Mo(1)–P(1)	133.39 (8)

[a] Prime indicates an atom with equivalent position coordinates $-x + {}^1/_2$, $-y + {}^1/_2, -z$.

Table IX. Interatomic Distances (Å) and Angles (deg) for $[PPN][Mo_6Se_8(PEt_3)_6]$ (**4**)

Mo(1)–Mo(1)′	3.837 (3)	Mo(2)–Mo(2)′	3.847 (3)
Mo(3)–Mo(3)′	3.829 (2)	Mo(1)–Mo(2)	2.712 (3)
Mo(1)–Mo(3)	2.707 (2)	Mo(1)–Mo(2)′	2.722 (3)
Mo(1)–Mo(3)′	2.714 (2)	Mo(2)–Mo(3)	2.720 (2)
Mo(2)–Mo(3)′	2.708 (2)	Mo(1)–Se(1)	2.561 (3)
Mo(1)–Se(2)	2.575 (3)	Mo(1)–Se(3)	2.566 (3)
Mo(1)–Se(4)	2.573 (3)	Mo(2)–Se(2)	2.566 (3)
Mo(2)–Se(4)	2.563 (3)	Mo(3)–Se(1)	2.574 (3)
Mo(3)–Se(4)	2.570 (3)	Mo(2)′–Se(1)	2.571 (3)
Mo(2)′–Se(3)	2.571 (3)	Mo(3)′–Se(2)	2.572 (3)
Mo(3)′–Se(3)	2.580 (3)	Mo(1)–P(1)	2.573 (6)
Mo(2)–P(2)	2.578 (6)	Mo(3)–P(3)	2.559 (6)
Mo(2)–Mo(1)–Mo(3)	60.26 (6)	Mo(3)–Mo(1)–Mo(3)′	89.88 (7)
Mo(2)–Mo(1)–Se(1)	118.68 (9)	Mo(2)′–Mo(1)–Se(1)	58.16 (7)
Mo(1)–Se(1)–Mo(2)′	64.06 (7)	Mo(2)–Mo(1)–P(1)	134.3 (1)

[a] Prime indicates an atom with the equivalent position coordinates $-x + {}^1/_2$, $-y + {}^1/_2, -z$.

solutions. In dichloromethane, an oxidation and a reduction process were observed, whereas in THF another reduction process could also be observed at lower potential (Table XII). Figure 4 shows a typical cyclic voltammogram of **1** in THF.

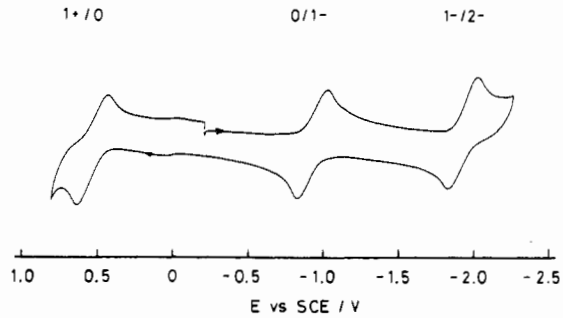

Figure 4. Cyclic voltammogram of $[Mo_6S_8(PEt_3)_6]$ (**1**) in THF.

Table X. Bond Distances (Å) in Complexes **1–4** and Chevrel Phases

compd	Mo–Mo: range (av)	Mo–S: range (av)	ref
$[Mo_6S_8(PEt_3)_6]$	2.662–2.664 (2.663)	2.44–2.45 (2.45)	this work
$[Mo_6Se_8(PEt_3)_6]$	2.697–2.708 (2.703)	2.55–2.57 (2.56)	this work
$[PPN][Mo_6S_8(PEt_3)_6]$	2.664–2.677 (2.670)	2.44–2.47 (2.46)	this work
$[PPN][Mo_6Se_8(PEt_3)_6]$	2.707–2.722 (2.714)	2.56–2.58 (2.57)	this work
Mo_6S_8	2.698–2.862 (2.780)	2.43–2.46 (2.44)	3b
Mo_6Se_8	2.684–2.836 (2.760)	2.55–2.59 (2.57)	3b
$AgMo_6S_8$	2.706–2.804 (2.755)	2.43–2.48 (2.45)	3b
$AgMo_6Se_8$	2.701–2.776 (2.738)	2.55–2.61 (2.58)	3b

The thin-layer coulometry of 1.2 mM solutions of **1** (ferrocene used as reference) indicated that each step was a one-electron redox process. The oxidation potentials for **1** and **2** in THF are 0.16 and 0.19 V more positive, respectively, as compared with the values in dichloromethane. The reason for the solvent effect is not clear. The scan rates were varied from 20 to 200 mV s^{-1}. The i_{pa}/i_{pc} values of the THF solutions were 1.0–1.1 for the first oxidation and reduction steps, but the ratio for the second reduction step was 0.71–0.73. These data imply the one-electron quasi-reversible redox processes[12] that are described as follows.

$$[Mo_6X_8(PEt_3)_6]^+ \underset{-e^-}{\overset{e^-}{\rightleftharpoons}} [Mo_6X_8(PEt_3)_6] \underset{-e^-}{\overset{e^-}{\rightleftharpoons}} [Mo_6X_8(PEt_3)_6]^- \underset{-e^-}{\overset{e^-}{\rightleftharpoons}} [Mo_6X_8(PEt_3)_6]^{2-}$$

X = S, Se

Discussion

Synthesis. Rational synthesis of cluster complexes is one of the most important fields in metal cluster chemistry.[13] It is generally expected that use of building blocks to construct cluster skeletons offers more selective preparations than starting from mononuclear complexes.[14] Bridging chalcogen atoms are especially useful to bind building blocks.[15] Although the idea itself is not new, the number of successful examples has been limited. Recently, novel hexanuclear complexes have been prepared from trinuclear[16] and dinuclear complexes.[17] Some octahedral cluster compounds have been prepared from trinuclear clusters.[18,19] The

(12) (a) Zanello, P. *Coord. Chem. Rev.* **1988**, *83*, 199. (b) Lemoine, P. *Coord. Chem. Rev.* **1988**, *83*, 169.
(13) (a) Vargas, M. D.; Nicholls, J. N. *Adv. Inorg. Chem. Radiochem.* **1986**, *30*, 123. (b) Roberts, D. A.; Geoffroy, G. L. *Comprehensive Organometallic Chemistry*; Wilkinson, G., Stone, F. G. A.; Abel, E. W., Eds.; Pergamon: Oxford, England, 1982; Chapter 40.
(14) Geoffroy, G. L. *Metal Clusters in Catalysis*; Gates, B. C., Guczi, L., Knözinger, H., Eds.; Elsevier: Amsterdam, 1986; Chapter 1.
(15) (a) Adams, R. D. *Polyhedron* **1985**, *4*, 2003. (b) Vahrenkamp, H. *Angew. Chem., Int. Ed. Engl.* **1975**, *14*, 322.
(16) Adams, R. D.; Babin, J. E. *Inorg. Chem.* **1987**, *26*, 980.
(17) Cotton, F. A.; Kibala, P. A.; Roth, W. J. *J. Am. Chem. Soc.* **1988**, *110*, 298.
(18) Johnson, B. F. G.; Johnston, R. D.; Lewis, J. *J. Chem. Soc. A* **1968**, 2865.
(19) (a) Perrin, C.; Sergent, M. *New J. Chem.* **1988**, *12*, 337. (b) Nanjundaswamy, K. S.; Vasanthacharya, N. Y.; Gopalakrishnan, J.; Rao, C. N. R. *Inorg. Chem.* **1987**, *26*, 4286.

Table XI. XPS and UV Data for Complexes $[Mo_6S_8(PEt_3)_6]$ (**1**) and $[Mo_6Se_8(PEt_3)_6]$ (**2**)

	binding energy/eV[a]				λ_{max}/nm[b] ϵ/M^{-1} cm^{-1}		
	Mo $3d_{5/2}$ Mo $3d_{3/2}$	S 2p	Se 3d	P 2p			
$[Mo_6S_8(PEt_3)_6]$	227.8	161.1, 162.1 (sh)		130.6	491	991	1200
	231.0				8.1×10^3	1.2×10^3	sh
$[Mo_6Se_8(PEt_3)_6]$	227.8			130.6	566	1034	1152
	230.8		53.8		5.5×10^3	1.4×10^3	sh

[a] C 1s: 284.6 eV. [b] Solvent: **1**, benzene; **2**, chloroform.

Table XII. Formal Potentials for Complexes $[Mo_6S_8(PEt_3)_6]$ (**1**) and $[Mo_6Se_8(PEt_3)_6]$ (**2**)[a]

		$E°$/V vs F_c/F_c^+		
	solvent	+1/0	0/−1	−1/−2
$[Mo_6S_8(PEt_3)_6]$	CH_2Cl_2	−0.23	−1.50	
	THF	−0.07	−1.50	−2.51
$[Mo_6Se_8(PEt_3)_6]$	CH_2Cl_2	−0.23	−1.50	
	THF	−0.05	−1.47	−2.45

[a] $E°(F_c/F_c^+)$ = 0.498 V (in CH_2Cl_2) and 0.595 V (in THF) vs NaSCE.

attempts to prepare molecular model compounds for the Chevrel phases by exchanging the face-bridging halides by chalcogenides have been partially rewarded.[20] The designed synthesis of octahedral Chevrel models by condensation of two triangular cluster units in the present study provides the first example of such synthesis, and this method has successfully been applied to the synthesis of tungsten analogues.[21]

Structure. Since the molybdenum cluster complexes studied in this work have no intercluster Mo–X bond as found in the solid-state Chevrel phases, the Mo–Mo bond distances should purely reflect the electronic factors of the molybdenum cluster and the effects of the chalcogen atoms. The Pauling bond order sum per electron PBO/e[22] values (eq 2) for complexes **1**–**4** are

$$d(\text{Mo–Mo}) = 2.619 - 0.60 \log n$$

$$\text{PBO/e} = 4 \times n/(20/6) \text{ for } \mathbf{1} \text{ and } \mathbf{2};\ 4 \times n/(21/6) \text{ for } \mathbf{3} \text{ and } \mathbf{4} \quad (2)$$

1.07, 0.87, 0.93, and 0.79, respectively. These values are comparable with those for a number of hexanuclear clusters[23] and indicate that the Mo–Mo distances are predominated by the number of the bonding electrons on the molybdenum atoms.

The results of the structure determinations show that the metal octahedra of the neutral complexes **1** and **2** are very regular, in contrast to the corresponding solid-state compounds Mo_6X_8 (X = S, Se, Te) that contain trigonally elongated Mo_6 octahedra. It is not unreasonable that no distortion is observed in the neutral complexes because the triply degenerate HOMO[2,24] is completely occupied in these 20-electron clusters.

The one-electron reduction of the neutral complex is accompanied by a slight elongation of the average metal–metal bond distance (0.11 (1) Å in **3** and 0.010 (1) Å in **4**), and a small distortion of the metal octahedron is found in the anionic complexes **3** and **4**. Because the changes are very small, the nature of the LUMO where the additional electron enters is nonbonding or slightly antibonding with respect to the metal–metal bonding. The small distortion of the metal octahedron may be explained in terms of Jahn–Teller effect for the partial occupation of the e_g orbital. Especially in the sulfido complex **3**, the main component of the distortion of the metal octahedron is the tetragonal elongation along the Mo(2)–Mo(2)′ axis: the distance Mo(2)–Mo(2)′ is longer than the other two metal–metal distances across the centers by 0.019 (2) Å (Table VIII).

The reduced complexes have molybdenum–chalcogen and molybdenum–phosphorus bond distances longer by 0.01–0.02 Å than those of the corresponding neutral complexes. These elongations can be attributed to the increase of the radius of the molybdenum due to the reduction. The elongation of the Mo–X bond distances on reduction is consistent with the result of the electronic structure calculation that the LUMO e_g orbital has Mo–X antibonding nature.[24a]

The Mo–Mo distances in the selenido complexes, **2** and **4**, are longer by 0.04 Å than those in the corresponding sulfido complexes, **1** and **3**. This elongation is associated with the larger van der Waals radius of selenium atom. Because the selenido ligands cannot approach each other as closely as sulfido ligands, they draw out the molybdenum atoms to which they are bonded. Similar effects have been observed in other chalcogenide and halide cluster compounds and have been termed as "matrix effects".[23]

As discussed above, the structures of the molecular chalcogenide cluster complexes are quite normal; i.e., the calculated PBO/e values are approximately equal to unity, the metal octahedral are regular for 20 electrons, and the replacement of sulfido ligands with selenido makes the metal–metal bond distances longer. In contrast, in the solid-state compounds, Mo_6X_8 and Chevrel phases $M_xMo_6X_8$, PBO/e values are much lower than unity, the clusters show trigonally elongated octahedra, and the selenides have shorter metal–metal bond distances than the sulfides. Yvon proposed that the trigonal elongation and the shorter bond distance of the selenides could be associated with the effective number of electrons in the metal cluster.[3] However, Corbett argued that these are due to the intercluster metal–chalcogen interactions on the basis of the discussion of the PBO/e values of many cluster compounds.[4] The present results clearly show that the number of electrons in the metal cluster alone cannot cause such structural features as found in the solid-state compounds because they are not observed in the molecular compounds with same number of electrons. On the other hand, the present results are completely consistent with Corbett's conclusion that these anomalies of the solid-state compounds are due to the intercluster interactions. In addition, in the metal octahedra in the solid-state compounds M_6X_8 with 20 electrons, the bands near the Fermi energy that corresponds to the HOMO and LUMO orbitals of the molecular complexes are not completely occupied due to the intercluster interaction. Such an electronic configuration may prefer the trigonal elongation of the metal octahedron as discussed by Nohl et al.[25]

The electronic effects in the solid-state compounds are often masked by strong intercluster interactions between the discrete cluster units. The structures of the molecular model compounds are necessary to estimate the contribution of the electronic effects to the structures of the solid-state cluster compounds with the same cluster units. This conclusion does not always ignore the importance of the electronic effects also in the solid-state M_6 cluster compounds. If other conditions such as intercluster bonding or

(20) (a) Michel, J. B.; McCarley, R. E. *Inorg. Chem.* **1982**, *21*, 1864. (b) Ebihara, M.; Toriumi, K.; Saito, K. *Inorg. Chem.* **1988**, *27*, 13.
(21) Saito, T.; Yoshikawa, A.; Yamagata, T.; Imoto, H.; Unoura, K. *Inorg. Chem.* **1989**, *28*, 3588.
(22) Pauling, L. *The Nature of the Chemical Bond*, 3rd ed.; Cornell University, Press: Ithaca, NY, 1960; p 400.
(23) Corbett, J. D. *J. Solid State Chem.* **1981**, *37*, 335.
(24) (a) Le Beuze, L.; Makhyoun, M. A.; Lissillour, R.; Chermette, H. *J. Chem. Phys.* **1982**, *76*, 6060. (b) Hughbanks, T.; Hoffmann, R. *J. Am. Chem. Soc.* **1983**, *105*, 1150. (c) Burdett, J. K.; Lin, J.-H. *Inorg. Chem.* **1982**, *21*, 5. (d) Bullett, D. W. *Phys. Rev. Lett.* **1977**, *39*, 664. (e) Mattheiss, L. F.; Fong, C. Y. *Phys. Rev. B.* **1977**, *15*, 1760. (f) Bronger, W.; Miessen, H.-J. *J. Less-Common Met.* **1982**, *83*, 29.
(25) Nohl, H.; Klose, W.; Andersen, O. Reference 2a, p 165.

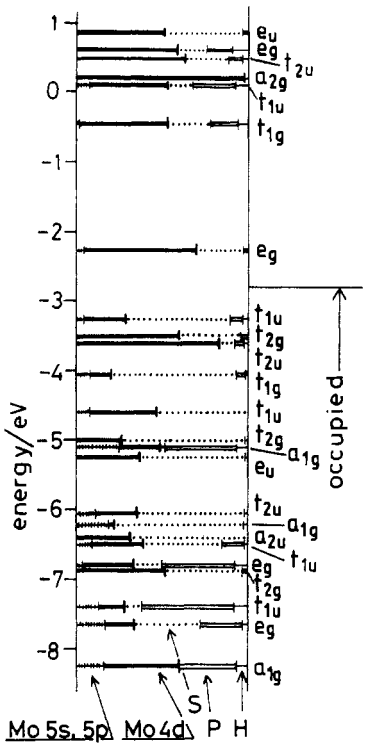

Figure 5. Electronic energy levels of $[Mo_6S_8(PH_3)_6]$ near the Fermi energy calculated by the DV-Xα method.[11] The contributions of each atomic orbital are indicated by different kinds of lines.

crystal packing allow, 24-electron clusters tend to show regular octahedral structures[26] and 23-, 22-,[27] and 21-electron clusters are distorted.

Spectra. The cluster complexes **1**–**4** show characteristic absorptions near 1000 and 500 nm (Table XI). The DV-Xα MO calculation of $[Mo_6S_8(PH_3)_6]$ by Imoto (Figure 5)[11] indicates that the HOMO of this 20-electron cluster complex is the t_{1u} orbital and the LUMO is the e_g orbital. The t_{2g} and t_{2u} orbitals have slightly lower energy than the t_{1u} orbital. The MO calculations on $[Mo_6S_8]^{2-}$ or $[Mo_6S_8]^{4-}$ show different level orders,[19] but our model is most closely related to complex **1** and it would be justifiable to correlate the spectra to the model. It is likely that the absorptions in the 1000-nm region are assignable to the $e_g \leftarrow t_{1u}$ transition. The energy gap in the calculation is 0.98 eV. The notably high molar extinction coefficients of the bands indicate that the transitions have a charge-transfer nature. This is consistent with the result of the calculation that the HOMO t_{1u} orbital is made mainly of sulfur p orbitals, and the LUMO e_g orbital, of molybdenum d orbitals (orbital contributions: t_{1u}, Mo 4 d 25%, S 3p 59%, P 3p 3%; e_g, Mo 4d 66%, S 3p 22%, P 3p 0%).

On reduction, the bands shift to somewhat lower energy. The binding energies of the molybdenum and phosphorus atoms in the XPS of **1** and **2** are almost identical, and the oxidation states of the cluster cores seem comparable.[28]

Electrochemistry. The potentials for the sulfido and selenido complexes are not very different, and the extent of charge transfer from face-bridging selenium atoms to the cluster core in **2** may be similar to that from sulfur in **1**. This is in accord with the result of the XPS (vide supra) and contradicts the view that the net charge transfer from the selenium atoms is larger than that from the sulfur atoms in the solid-state Chevrel phases.[3]

The cluster complexes **1** and **2** show redox chemistry similar to that of $[M_6S_8(PEt_3)_6]$ (M = Fe, Co),[29] but the filling of the LUMO in the 20-electron molybdenum cluster complexes is more difficult. The one-electron-reduced clusters **3** and **4** are extremely sensitive to oxidation, and the preparation of more reduced species would be formidable.

Conclusion

The results of the present study have demonstrated that the 20-electron molecular cluster complexes **1** and **2** have regular octahedral cores. This is due to the virtual lack of intercluster Mo–X interaction and the absence of Jahn–Teller type distortion in **1** and **2**. The selenido derivative **2** has Mo–Mo and Mo–X bond distances longer than those of the sulfido derivative **1**. A slight distortion of the octahedra occurs on one-electron reduction of the complexes, and the average Mo–Mo and Mo–X bond distances become longer. The standard redox potentials are very similar for **1** and **2**. The data conform to the small difference of the electronegativities of sulfur and selenium,[30] and the net charge transfer from the eight chalcogen atoms should be similar. The longer Mo–Mo and Mo–Se bond distances in **2** as compared with those in **1** can be explained by the longer bond radius of the selenium atom. Because there is no anomaly in the molecular model complexes, the anomalous structural features in the solid-state Chevrel phases, at least in the simplest Mo_6X_8 (X = S, Se) compounds, can be interpreted in terms of the strong intercluster Mo–X bonding.[31]

Acknowledgment. Support from the Ministry of Education, Science and Culture of Japan (Grant-in-Aid for Special Project Research No. 62115007 and for General Research No. 63430010) and the Iwatani Naoji Foundation's Research Grant is gratefully acknowledged. We thank Nippon Chemical Co. Ltd. for the gift of triethylphosphine.

Supplementary Material Available: A detailed list of X-ray data collection conditions (Table SI), thermal parameters of **1**–**4** (Tables SII–SV), atomic parameters of fixed hydrogen atoms of **1** (Table SVI), and complete bond distances and angles of **1**–**4** (Tables SVII–SX) (17 pages); listings of observed and calculated structure factors (51 pages). Ordering information is given on any current masthead page.

(26) Bronger, W.; Fleishhauer, J.; Marzi, H.; Raabe, G.; Schleker, W.; Schuster, T. *J. Solid State Chem.* **1987**, *70*, 29.
(27) Stollmaier, F.; Simon, A. *Inorg. Chem.* **1985**, *24*, 168.
(28) Yashonath, S.; Hegde, M. S.; Sarode, P. R.; Rao, C. N. R.; Umarji, A. M.; Subba Rao, G. V. *Solid State Commun.* **1981**, *37*, 325.
(29) (a) Cecconi, F.; Ghilardi, C. A.; Midollini, S.; Orlandini, A. *J. Chem. Soc., Dalton Trans.* **1987**, *831*. (b) Agresti, A.; Bacci, M.; Cecconi, F.; Ghilardi, C. A.; Midollini, S. *Inorg. Chem.* **1985**, *24*, 689. (c) Cecconi, F.; Ghilardi, C. A.; Midollini, S.; Orlandini, A.; Zanello, P. *Polyhedron* **1986**, *5*, 2121.
(30) (a) Sen, K. D., Jørgensen, C. K., Eds. *Electronegativity*; Structure and Bonding, Vol. 66; Springer: Berlin, 1987. (b) Pearson, R. G. *Inorg. Chem.* **1988**, *27*, 734.
(31) Note added in proof: Recently, Kubel and Yvon reported that, in isoelectronic ternary phases MMo_6S_8 (M = Yb^{2+}, Eu^{2+}, Sr^{2+}, Ba^{2+}, Ca^{2+}), the Mo–Mo intracluster bonds correlate with matrix effect. See: Kubel, F.; Yvon, K. *J. Solid State Chem.* **1988**, *73*, 188.